N-Nitrosation of Amines by NO_2 and NO: A Theoretical Study

Yi-Lei Zhao,*[,†,‡,#] Stephen L. Garrison,[†,‡,#] Carlos Gonzalez,*[,†] William David Thweatt,[‡,§,#] and Manuel Marquez*[,†,§,||]

NIST Center for Theoretical and Computational Nanosciences, National Institute of Standards and Technology, 100 Bureau Drive MS 8380, Gaithersburg, Maryland 20899, Philip Morris Interdisciplinary Network of Emerging Science and Technology (INEST) Group, Philip Morris, 4201 Commerce Road, Richmond, Virginia 23234, Philip Morris Research Center, 4201 Commerce Road, Richmond, Virginia 23234, and Harrington Department of Bioengineering, Arizona State University, Tempe, Arizona 85287

Received: November 22, 2006; In Final Form: January 23, 2007

Gas-phase nitrosation of amines implies a nonionic pathway different from the nitrosonium nitrosation via acidification of nitrite. Electronic structure calculations discussed in this work suggest a free radical mechanism, in which NO_2 abstracts a hydrogen atom from the nitrogen in primary and secondary amines to form an intermediate complex of an aminyl radical and nitrous acid. The aminyl radical intermediate is then quenched by nitric oxide, leading to the formation of nitrosamine. High-level calculations (CBS-QB3) show that alkyl substitutions on amines can activate the H-abstraction reaction. Thus, while H-abstraction from NH_3 was found to exhibit a reaction barrier ($\Delta H^{\ddagger}$) of 106 kJ/mol, similar calculations indicate that the corresponding barriers decrease to 72 and 45 kJ/mol for methylamine and dimethylamine, respectively. Heterocyclic secondary amines have also been investigated in a similar manner. The five-membered-ring (5-m-r) amine appears to be the most reactive: pyrrolidine ($\Delta H^{\ddagger} = 30$ kJ/mol), azetidine ($\Delta H^{\ddagger} = 44$ kJ/mol), piperidine ($\Delta H^{\ddagger} = 44$ kJ/mol), and aziridine ($\Delta H^{\ddagger} = 74$ kJ/mol). The reaction barrier for 1*H*-pyrrole, an aromatic 5-m-r secondary amine, was found to be 59 kJ/mol. The origin of the high activity for the 5-m-r alkylamine stems from a hydrogen-bond-like interaction between the aminyl radical and the nascent nitrous acid molecule. This theoretical study suggests that, in the presence of nitrogen oxides, the gas-phase nitrosation of secondary amines is feasible.

Introduction

N-Nitrosamines, thought to be toxic and carcinogenic,[1−3] are found in a number of environments, e.g., as contaminants in malt beverages[4] and foods treated with nitrites,[5] in the manufacture of rubber,[6] in cigarette smoke, and in treated wastewater.[7] *N*-Nitrosamines are formed from secondary amines and nitrogen oxides in air or lipid.[8,9] As such, it is important to understand the formation mechanisms of *N*-nitrosamines in order to reduce their presence in the environment.

In the laboratory, *N*-nitrosamines are traditionally prepared by the reaction of secondary amines with nitrous acid formed in situ under aqueous acidic conditions.[10,11] Nitrosonium ion (H_2ONO^+, protonated nitrous acid) nitrosates secondary amines via a series of proton/nitrosonium transfers. Although the nitrosation of nitrite-slated foodstuffs in the stomach is believed to follow this mechanism,[12] it cannot explain the nitrosation of amines in the gas phase or in nonpolar solvents, given the absence of a polar environment necessary to stabilize the ionic intermediate species. For example, in rubber and food industries,[13−21] several studies have indicated that nitrosamines can be generated from amines in the gas, lipid, and even condensed phase.[22] Certain studies have suggested that nitrogen oxides play an important role in some nitrosation reactions.[8] These results suggest that nitric oxide (NO) and nitrogen dioxide (NO_2) most likely play a role in nitrosation reactions.

The acid-catalyzed nitrosation mechanism is unlikely to occur in the gas phase due to a lack of solvent molecules necessary to stabilize the intermediate ions. The gas-phase nitrosation of secondary amines by NO_2−NO that is observed experimentally must undergo an alternative pathway, even though nitrosonium donors such as N_2O_3 and N_2O_4 are likely present. Previous research in combustion processes has shown that ammonia can react with NO and NO_2 at high temperatures.[23] In NH_3 de-NO_x chemistry and high-energy material science, a number of experiments have been conducted dealing with the reactions of NO_x plus NH_x.[24] However, mechanistic details of these reactions are difficult to extract from the experimental data currently available. Mebel et al. investigated the H-abstraction reaction from NH_3 with NO and NO_2 computationally.[25,26] Compared to the high H-abstraction barriers by NO leading to HNO (ca. 220 and 260 kJ/mol at the MP2 and G2 levels of theory, respectively),[27] conversion of NO_2 to HONO via a similar H-abstraction mechanism is significantly more feasible. However, the H-abstraction by NO_2 was found to be conformation-

* Corresponding Authors. E-mail: yilei.zhao@nist.gov (Y.-L.Z.); Carlos.gonzalez@nist.gov (C.G.); Manuel.M.Sanchez@pmusa.com (M.M.); Telephone: (301)975-2111 (Y.-L.Z.); (301)975-4063 (C.G.); (804)274-5195 (M.M.).

† NIST Center for Theoretical and Computational Nanosciences.

‡ Philip Morris Interdisciplinary Network of Emerging Science and Technology (INEST) Group.

§ Philip Morris Research Center.

|| Harrington Department of Bioengineering.

Philip Morris Interdisciplinary Network of Emerging Science and Technology (INEST) fellow.

10.1021/jp0677703 CCC: $37.00
Published on Web 03/01/2007

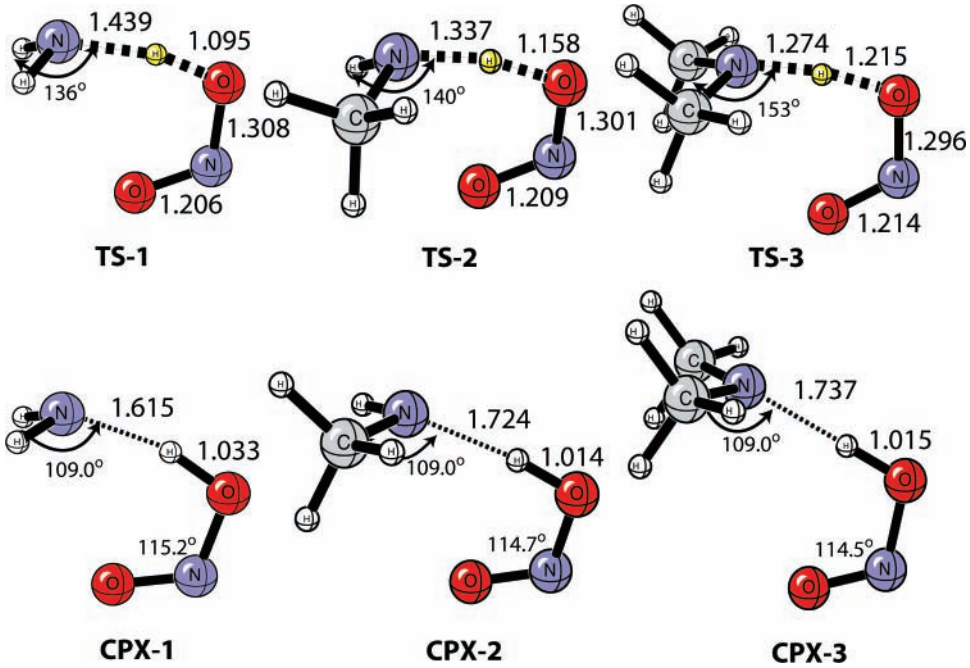

Figure 1. The transition states and the hydrogen-bonding intermediates of ammonia, methylamine, and dimethylamine reacting with NO_2, from the CBS-QB3 method. (distance in Å, angles referring to R−N−R planes).

dependent, similar to the case of O−O cleavage in HOONO.[28] The cis-conformation transition state leading to HNO_3 was predicted by DFT, UMP2, QCISD(T), and G1 calculations to be lower in energy by 36−56 kJ/mol than the trans-conformation. These results correlate well with the fact that, while the NO_2 moiety in the cis-conformation transition state (TS) adopts the $^2A_1$ electronic state (N-centered radical), the NO_2 moiety in the trans-conformation TS is found in the relatively higher-energy $^2B_2$ electronic state (O-centered radical).

Nitrogen dioxide can also abstract hydrogen atoms from primary and secondary amines. The resulting aminyls ($\bullet NH_2$, $\bullet NHMe$, $\bullet NMe_2$) are highly reactive agents that will likely be scavenged by the most abundant radicals existent in the system. At relatively high concentrations of NO, this will lead to formation of nitrosamines. In the case of secondary amines, the resulting nitrosodialkylamines are more stable than the H_2NNO and RNHNO species from NH_3 and primary amines, which can further decompose to N_2 and water/alcohol. ($H_2NN{=}O \rightarrow HN{=}NOH \rightarrow N_2 + H_2O$, and $RNHNO \rightarrow RN{=}NOH$).

In this work, we present a novel radical mechanism for gas-phase nitrosation that is in qualitative agreement with previous experiments describing the nitrosation of secondary amines by nitrogen oxides under basic condition (pH 8.5).[29]

Computational Method

Density functional theory (DFT) calculations were performed with the three-parameter hybrid B3LYP exchange-correlation functional using the 6-31+G* basis set[30] (herein the B3LYP/6-31+G* level of theory). All calculations were carried out with the Gaussian03 suite of programs.[31] The nature of every stationary point was verified by harmonic vibrational frequency analysis at the B3LYP/6-31+G* level. These stationary points were then re-optimized using the CBS-QB3 method by Petersson et al.,[32] known to exhibit a mean error of 4 kJ/mol with respect to the G2 experimental data set. In the Supporting Information, the free energies in solution were calculated at the B3LYP/CBSB7 level using the CPCM-polarizable continuum method[33] and added to the gas-phase CBS-QB3 energies to model nitrosation by nitrite acidification.

TABLE 1: CBS-QB3 Energies, Enthalpies, Entropies, and Gibbs Free Energies (at 298 K and 1 atm) for All Stationary Points Considered in This Study[a]

species	$E^{(0K)}_{CBS}$	H^{298K}_{CBS}	S	G^{298K}_{CBS}
NH_3	−56.457	−56.456	46.0	−56.478
$MeNH_2$	−95.665	−95.664	57.4	−95.691
Me_2NH	−134.880	−134.879	64.9	−134.910
NO	−129.746	−129.745	49.0	−129.768
NO_2	−204.850	−204.849	58.7	−204.877
TS-1	−261.265	−261.264	71.5	−261.299
TS-2	−300.486	−300.485	81.8	−300.524
TS-3	−339.712	−339.711	91.2	−339.754
CPX-1	−261.266	−261.265	75.1	−261.301
CPX-2	−300.491	−300.490	89.2	−300.532
CPX-3	−339.718	−339.717	94.2	−339.762
H_2NNO	−185.609	−185.608	61.3	−185.638
cis-MeNHNO	−224.831	−224.830	69.2	−224.863
trans-MeNHNO	−224.829	−224.828	68.8	−224.860
Me_2NNO	−264.053	−264.052	72.7	−264.087
$H_2N^\bullet$	−55.788	−55.787	47.9	−55.810
$MeHN^\bullet$	−95.008	−95.007	58.5	−95.035
$Me_2N^\bullet$	−134.232	−134.232	69.5	−134.265
cis-HONO	−205.471	−205.470	59.1	−205.498
trans-HONO	−205.472	−205.471	59.3	−205.499

[a] Energies, Enthalpies, and Gibbs Free Energy in Hartrees (1 Hartree = $4.3597482 \times 10^{-18}$ Joules Per Particle = 2.6255×10^3 kJ/mol), and Entropies in esu (1 esu = 4.184 J/mol-K).

Results

Figure 1 shows the fully optimized geometries for the transition structures involving H-abstraction reactions by NO_2 from ammonia (**TS-1**) as well as from the primary (**TS-2**) and secondary amine (**TS-3**) considered in this study. In addition, the optimized geometries of the corresponding hydrogen-bonded complexes (**CPX-1**, **CPX-2**, and **CPX-3**) afforded by these transition structures are also shown in Figure 1. The optimized structures of other stationary points such as the reactants and products are provided in the Supporting Information. In addition, Table 1 lists the CBS-QB3 energies, enthalpies, entropies, and free energies calculated at 298.15 K and 1 atm of pressure for all stationary points considered in this study. All energy

TABLE 2: CBS-QB3 Reaction Energies and Activation Energies (in kJ/mol) for the H-Abstractions and Radical Combinations in the Gas Phase

reaction	ΔH_{rxn}	ΔG_{rxn}	$\Delta H^{\ddagger}$
$NH_3 + NO_2 \rightarrow [H_2N\text{---}HONO]$	104.6	141.4	106.5
$CH_3NH_2 + NO_2 \rightarrow [CH_3NH\text{---}HONO]$	60.8	94.2	71.6
$(CH_3)_2NH + NO_2 \rightarrow [(CH_3)_2N\text{---}HONO]$	28.9	65.4	44.8
$[H_2N\text{---}HONO] + NO \rightarrow H_2NNO + HONO$	−180.7	−176.3	
$[CH_3NH\text{---}HONO] + NO \rightarrow$ *cis*-$CH_3NHNO + HONO$	−173.2	−161.0	
$[CH_3NH\text{---}HONO] + NO \rightarrow$ *trans*-$CH_3NHNO + HONO$	−167.2	−154.5	
$[(CH_3)_2N\text{---}HONO] + NO \rightarrow (CH_3)_2NNO + HONO$	−159.9	−145.9	

SCHEME 1: ROHF/6-31+G* Orbital Energies of the B1 (Singly Occupied) and A1 (Doubly Occupied) Orbitals

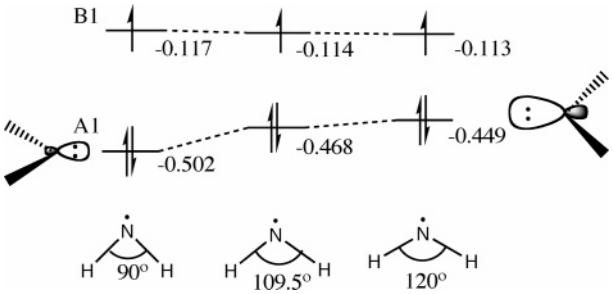

calculations are based on the CBS-QB3 thermochemistry scheme in Gaussian,[32b] where the thermodynamic properties include only electronic energy and thermal corrections. The computed heats of reaction (ΔH_{rxn}), Gibbs free energy of reaction (ΔG_{rxn}), as well as reaction barriers ($\Delta H^{\ddagger}_{CBS-QB3}$, corrected by zero point energy), are listed in Table 2.

Transition Structures and Barriers. The trends in the N−H bond-length reduction and the O−H bond-lengh elongation observed in Figure 1 for the transition structures indicate that alkylation of the amines leads to "earlier" transition states. The partially forming O−H bond lengths are predicted to be 1.095, 1.158, and 1.215 Å, in TS-1, TS-2, and TS-3, respectively, while the partially breaking N−H bond lengths were found to be 1.438, 1.337, and 1.274 Å (see Figure 1). The structures in Figure 1 also show that the ∠N−O(H)−N bending angle as well as the ∠R1−N−H−R2 dihedral angle (R1 and R2 = H, CH_3) become larger with alkylation (∠N−O(H)−N = 97.7°, 101.5°, and 103.3°, and ∠R1−N−H−R2 = 124.7°, 131.5°, and 148.5°, for **TS-1**, **TS-2**, and **TS-3**, respectively). Accordingly, a systematic increase in the angle between the R−N−R plane and the N−H bond is observed (136°, 140°, 153°, for **TS-1**, **TS-2**, and **TS-3**, respectively). The trends in this angle, ∠N−O(H)−N, and ∠R1−N−H−R2 indicate that alkylation of the amine induces changes in the hybridization of the amine's nitrogen atom in the transition state (possibly due to steric repulsions).

The results in Table 2 indicate that the reaction barrier for the H-abstraction process by NO_2 decreases with alkyl substitution by about 28−35 kJ/mol per alkyl group (barriers: 106 kJ/mol for NH_3, 72 kJ/mol for CH_3NH_2, and 45 kJ/mol for $(CH_3)_2NH$). This is consistent with changes in the N−H bond dissociation energies (BDE) in NH_3, CH_3NH_2, and $(CH_3)_2NH$ (450 kJ/mol for NH_3, 419 kJ/mol for CH_3NH_2, and 395 kJ/mol for $(CH_3)_2NH$; computed at the CBS-QB3 level of theory). Alkyl substitution can stabilize the transition structures by σ-donating electron density to the aminyl group.

Hydrogen-Bonding Complexes. The transition structures **TS-1**, **TS-2**, and **TS-3** lead directly to the formation of the hydrogen-bonding complexes **CPX-1**, **CPX-2**, and **CPX-3**, respectively (see Figure 1). Full geometry optimization of these complexes predict N---H distances of 1.615, 1.724, and 1.736 Å for **CPX-1**, **CPX-2**, and **CPX-3**, respectively. The results in Table 2 indicate that formation of these complexes from the parent amine, R_2NH (R═H, CH_3), and NO_2 is an endothermic process, in agreement with the fact that these reactions exhibit "early" transition structures (see discussion in previous section). In addition, it is observed that alkylation decreases the endothermicity of these reactions (see Table 2), leading to a more stable hydrogen-bonding complex (ΔH_{rxn} = 105, 61, and 29 kJ/mol, respectively, for the reactions affording **CPX-1**, **CPX-2**, and **CPX-3**, respectively). This trend is the result of the ability of the incipient aminyl moiety in the complex to bind more strongly to the HONO moiety with increasing alkyl substitution. This is consistent with the heats of reaction trends observed in the following decomposition reactions:

$$\textbf{CPX-1} \rightarrow \bullet NH_2 + HONO \qquad \Delta H_{rxn} = 18.3 \text{ kJ/mol} \quad \text{(R1)}$$

$$\textbf{CPX-2} \rightarrow \bullet NHMe + HONO \qquad \Delta H_{rxn} = 30.5 \text{ kJ/mol} \quad \text{(R2)}$$

$$\textbf{CPX-3} \rightarrow \bullet NMe_2 + HONO \qquad \Delta H_{rxn} = 38.4 \text{ kJ/mol} \quad \text{(R3)}$$

These trends can be rationalized based on molecular orbital theory arguments. Alkylation on the nitrogen atom enlarges the R−N−R bending angle and gives the lone pair orbital (with A_1 symmetry) a larger 2p character, pushing its orbital energy ϵ_i up, as shown in Scheme 1. These lone pair orbitals become more diffuse with alkylation, increasing the hydrogen-bonding donor character of the aminyl moiety and leading to a stronger hydrogen bond in the complex.

Recombination of Aminyl and Nitric Oxide. When the concentration of nitric oxide is high enough, the nascent complexes **CPX-1**, **CPX-2**, and **CPX-3** can be scavenged by the excess NO, leading to the formation of nitrosamines. The reaction is driven by the NO attack on the unpaired electron occupying the B_1 orbital in the complex (see Scheme 1). Given

SCHEME 2: Radical Recombination of the Hydrogen-Bonding Intermediate with Nitric Oxide

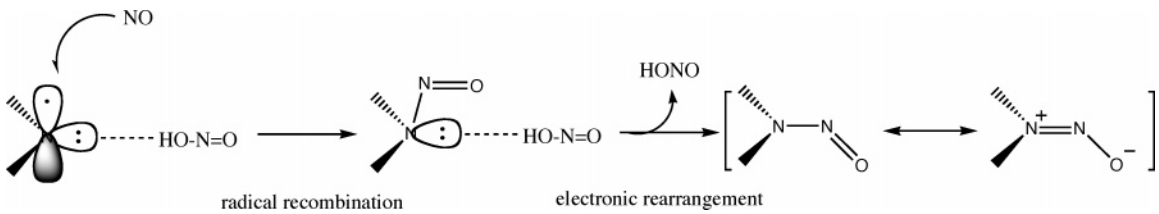

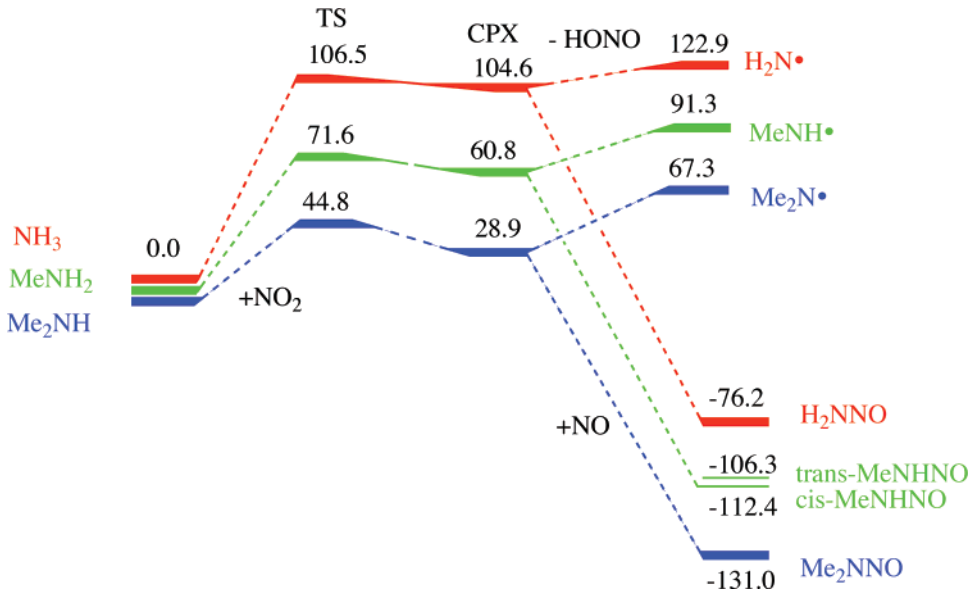

Figure 2. Diagram of the reaction enthalpy (in kJ/mol) in the gas phase for ammonia, methylamine, and dimethylamine reacting with NO_2-NO, from the CBS-QB3 method.

that the B_1 orbital is orthogonal to the A_1 lone pair orbital participating in the hydrogen bond with HONO, the radical recombination with nitric oxide affects the hydrogen bond neither geometrically nor electronically. Once the two nitrogen atoms approach each other at a distance short enough to form a single covalent bond, electronic rearrangements transform the incipient N−N single bond to a N═N−O conjugated bond, breaking the hydrogen bond between the aminyl and the HONO moieties (see Scheme 2). The energy stabilization gained from the N═N−O conjugation more than compensates for the energy increase involved in breaking the hydrogen bond.

The diagram shown in Figure 2, summarizes the energetics of the reactions of the amines NH_3, $MeNH_2$, and Me_2NH with NO_2/NO as discussed above. This diagram indicates that once the hydrogen-bonding complex is formed (**CPX-1**, **CPX-2**, and **CPX-3**), the recombination of the free aminyl radical moiety in the complex and nitric oxide is thermochemically favored over the direct decomposition of the hydrogen-bonding complexes. Only at high temperatures can these two pathways be expected to be competitive.

***N*-Nitrosamine Formation from Heterocyclic Secondary Amines.** Because heterocyclic secondary amines are ubiquitous as flavor compounds in food, we also studied them in a similar manner to assess their propensity to form *N*-nitrosamines in the presence of nitrogen oxides. Five heterocyclic amines were considered in this study: aziridine, azetidine, pyrrolidine, piperidine, and 1*H*-pyrrole, as representatives of 3-, 4-, 5-, and 6-m-r and aromatic amines, respectively. The optimized structures of the amines and their corresponding transition structures for the H-abstraction pathway are shown in Figure 3. The computed reaction barriers and N−H BDEs of the heterocyclic amines are listed in Tables 3 and 4.

Overall, the energy barriers exhibited by the H-abstraction reactions between NO_2 and the five heterocyclic amines considered in this study (Table 4) are comparable to the corresponding barriers computed for the acyclic amines (Table 2), indicating that N-nitrosation of heterocyclic amines is also possible. The results in Table 4 indicate that the H-abstraction barrier for aziridine (**TS-4**) is higher by 30 kJ/mol than the barrier for azetidine (**TS-5**) despite similar N−H BDEs of the parent amines. This result can be rationalized in terms of the existence of a less diffuse lone pair in the case of aziridine, which decreases the hydrogen bond donor character of the aziridinyl moiety in **TS-4**, leading to a less stable transition structure. This is supported by a smaller C−N−C angle in **TS-4**, compared to **TS-5** (61.3° vs 91.3°). In turn, the H-abstraction barrier in the case of pyrrolidine (**TS-6**) was found to be approximately 14 kJ/mol lower than the corresponding barrier for azetidine, probably due to pyrrolidine's lower N−H bond dissociation energy (Table 4) and larger C−N−C angle at the TS (109.8° vs 91.3°). It is interesting to notice that, in the case of the six-membered ring piperidine (Figure 3), the reaction barrier is approximately 15 kJ/mol higher than the barrier corresponding to the five-membered ring pyrrolidine despite exhibiting a larger C−N−C angle in its transition structure (**TS-7**). This increase in the barrier height is likely the result of piperidine's larger N−H BDE (Table 4).

The geometry optimizations performed in this work indicate a C−N−C bond angle change of 5° in the pyrrolidine moiety when going from the reactant to the transition state (104.8° vs 109.8°, see Figure 3), while the corresponding changes in the case of aziridine, azetidine, and piperidine were found to be significantly less (<2°) when proceeding from the amines (60.6°, 90.5°, and 112.3°, respectively) to the corresponding transition states (61.3°, 91.3°, and 114.4°, respectively). The larger change in the C−N−C angle in the case of pyrrolidine is due to the fact that, while the nitrogen atom prefers a pyramidal configuration in the reactants (pyrrolidine), a planar configuration is favored in the aminyl moiety of the transition state (see Scheme 3). It is this change in configuration adopted by the nitrogen atom in pyrrolidine that induces a larger stabilization of the transition structure, resulting in a lower barrier height than those for the other secondary amines considered in this study.

Compared to pyrrolidine, the H-abstraction from the aromatic five-membered ring amine 1*H*-pyrrole exhibits a barrier height approximately 29 kJ/mol larger (Table 4). The relatively large barrier in the case of 1*H*-pyrrole is the result of significant conjugation of the nitrogen's lone pair with the π-electrons in the aromatic ring, which stabilizes the reactant and weakens the hydrogen bond with the HONO moiety in the transition state. Geometry optimizations predict changes in the bond lengths of $N-C_\alpha$, $C_\alpha-C_\beta$, and $C_\beta-C_{\beta'}$ from 1.374, 1.376, and 1.424 Å, respectively, in the aromatic amine to 1.337, 1.441, and 1.376 Å, respectively, in the transition state (**TS-8** in Figure 3).

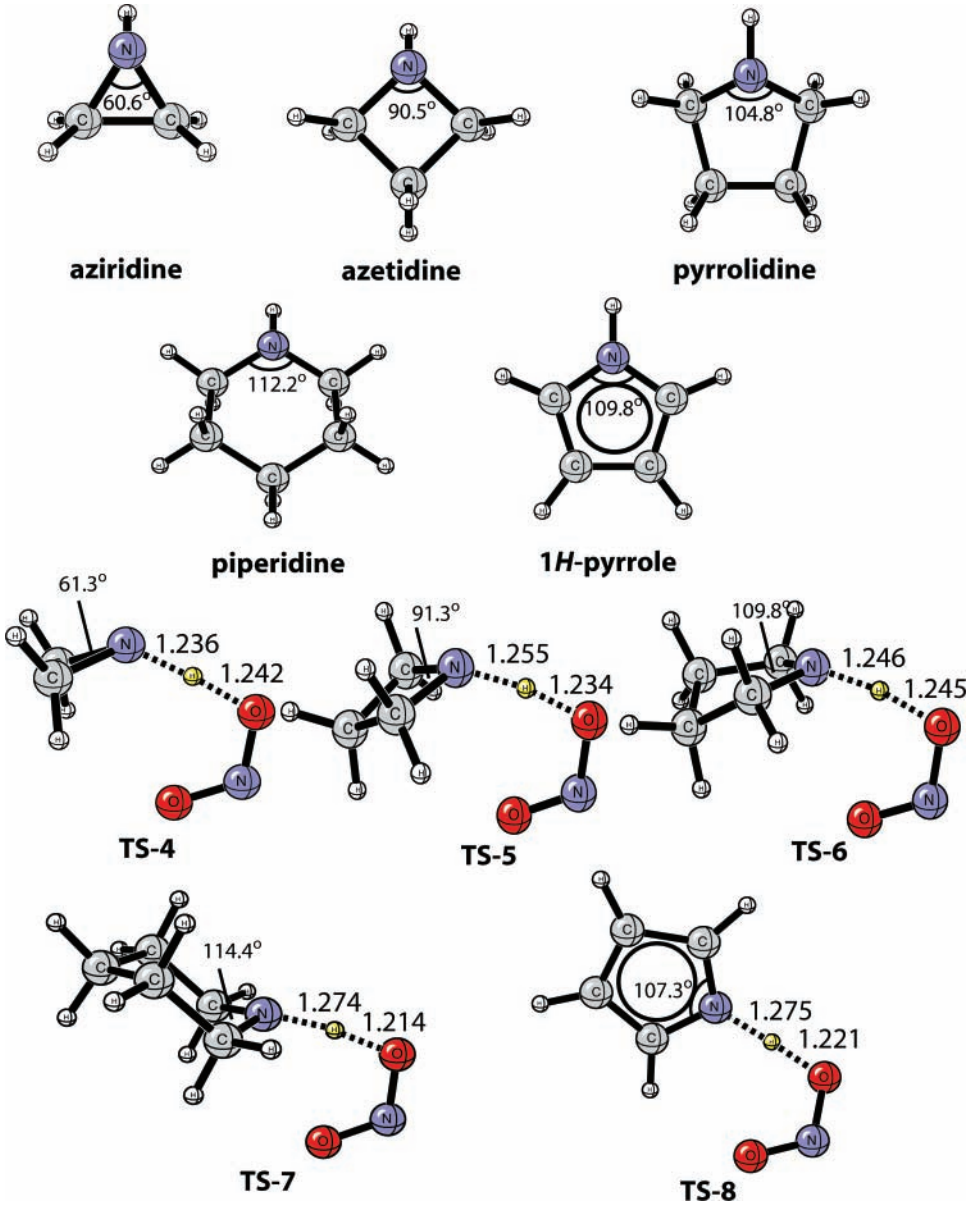

Figure 3. Optimized global minima and transition structures of N-nitrosation for aziridine, azetidine, pyrrolidine, piperidine, and 1*H*-pyrrole, from CBS-QB3 calculations.

TABLE 3: Computed Energies, Enthalpies, Entropies, and Free Energies at 298 K and 1 atm, with the CBS-QB3 Method in the Gas Phase (Using the Same Units as in Table 1)

species	*E*	*H*	*S*	*G*
$(CH_2)_2NH$ (aziridine)	−133.664	−133.663	59.7	−133.691
$(CH_2)_3NH$ (azetidine)	−172.891	−172.890	65.3	−172.921
$(CH_2)_4NH$ (pyrrolidine)	−212.147	−212.146	71.6	−212.180
$(CH_2)_5NH$ (piperidine)	−251.380	−251.379	73.9	−251.415
$(CH)_4NH$ (1*H*-pyrrole)	−209.782	−209.782	65.9	−209.813
TS-4	−338.484	−338.483	83.0	−338.523
TS-5	−377.723	−377.722	88.3	−377.764
TS-6	−416.984	−416.983	93.5	−417.028
TS-7	−456.212	−456.211	98.7	−456.258
TS-8	−414.609	−414.608	89.7	−414.650
$(CH_2)_2N^\bullet$	−133.016	−133.015	60.9	−133.044
$(CH_2)_3N^\bullet$	−172.243	−172.242	67.7	−172.274
$(CH_2)_4N^\bullet$	−211.503	−211.502	71.7	−211.536
$(CH_2)_5N^\bullet$	−250.731	−250.730	75.8	−250.766
$(CH)_4N^\bullet$	−209.132	−209.131	67.0	−209.163

TABLE 4: CBS-QB3 Reaction Barriers for H-Abstraction of the Heterocyclic Amines by Nitrogen Dioxide and Corresponding N−H Bond Dissociation Energy in the Gas Phase (in kJ/mol)

reaction	$\Delta H^\ddagger$
$(CH_2)_2NH + NO_2 \rightarrow [(CH_2)_2N\text{---}\ HONO]$	74.0
$(CH_2)_3NH + NO_2 \rightarrow [(CH_2)_3N\text{---}\ HONO]$	43.5
$(CH_2)_4NH + NO_2 \rightarrow [(CH_2)_4N\text{---}\ HONO]$	29.6
$(CH_2)_5NH + NO_2 \rightarrow [(CH_2)_5N\text{---}\ HONO]$	44.4
$(CH)_4NH + NO_2 \rightarrow [(CH)_4N\text{---}\ HONO]$	59.0
	BDE
$(CH_3)_2NH \rightarrow (CH_3)_2N^\bullet + H^\bullet$	394.7
$(CH_2)_2NH \rightarrow (CH_2)_2N^\bullet + H^\bullet$	393.8
$(CH_2)_3NH \rightarrow (CH_2)_3N^\bullet + H^\bullet$	395.2
$(CH_2)_4NH \rightarrow (CH_2)_4N^\bullet + H^\bullet$	384.2
$(CH_2)_5NH \rightarrow (CH_2)_5N^\bullet + H^\bullet$	399.7
$(CH)_4NH \rightarrow (CH)_4N^\bullet + H^\bullet$	401.5

Conclusion

Highly correlated ab initio molecular orbital calculations have been used to study the gas-phase N-nitrosation of a series of acyclic and heterocyclic amines. The results indicate a novel radical mechanism initiated by a hydrogen abstraction from the amine by nitrogen dioxide. In the case of the acyclic amines, it was found that alkylation leads to lower reaction barriers and more stable hydrogen-bonded complexes between the corre-

SCHEME 3: Pyrrolidine, Pyrrolidyl, 1*H*-pyrrole and 1*H*-pyrolyl

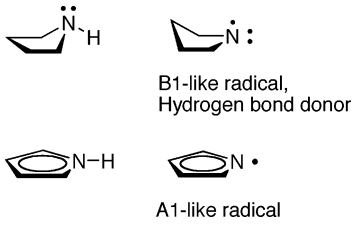

sponding aminyl radical and HONO. The stability of the complexes and transition structures was found to be the result of relatively low N−H bond dissociation energies as well as an increase in the donor character of the lone pair in the incipient aminyl radical moiety being formed. The results also show that, in an excess of NO, these complexes can readily react to form nitrosamines. Similar trends are observed in the case of the five hetrocyclic amines considered in this study. Because of their relatively lower barrier heights, it is expected that N-nitrosation of the heterocyclic amines will be more favorable from a thermochemical point of view than the corresponding N-nitrosation of the acyclic amines. This is particularly true in the case of NO_2 reacting with the five-membered-ring heterocyclic secondary amine pyrrolidine, which exhibits a barrier height approximately 15 kJ/mol lower than the barrier corresponding to the reaction between NO_2 and the acyclic secondary amine dimethylamine. These results suggest the possibility of controlling the production of nitrosamines in processes such as food preparation and rubber manufacture (where heterocyclic amines such as pyrrolidine can exist at significant concentrations) by limiting the concentration of NO_2 to significantly low levels.

Finally, the results of this work indicate that there exists a competing radical mechanism for the gas-phase nitrosation of secondary amines, especially for heterocyclic secondary amines. Under acidic conditions (such as pH = 2), the fast acid−base equilibrium catalyzes nitrosonium nitrosation, while in alkaline solutions, lipids, and gas phase, the acid-catalyzed nitrosation will be suppressed and the radical mechanism is likely to take place in the presence of nitrogen oxides.

Acknowledgment. Y.L.Z., S.L.G., and W.D.T. are Philip Morris Interdisciplinary Network of Emerging Science and Technology (INEST) fellowship recipients. We are grateful to Philip Morris USA for financial support of this research and to NIH and NIST for computer time. This study utilized the high-performance computational capabilities of the Biowulf PC/Linux cluster at the National Institutes of Health, Bethesda, MD (http://biowulf.nih.gov).

Supporting Information Available: Nitrosation mechanism in aqueous solution; geometries (*xyz* coordination); reaction potential energy surface of radical combination. This material is available free of charge via the Internet at http://pubs.acs.org.

References and Notes

(1) Magee, P. N.; Barnes, J. M. *Br. J. Cancer* **1956**, *10*, 114−122.

(2) *Scientific and Technical Assessment Report on Nitrosamines*; EPA-600/6-77-001; U.S. Environmental Protection Agency: Research Triangle Park, NC, 1977.

(3) Ichinose, T.; Fujii, K.; Sagai, M. *Toxicology* **1991**, *67*, 211−225.

(4) Izquierdo-Pulido, M.; Barbour, J. F.; Scanlan, R. A. *Food Chem. Toxicol.* **1996**, *34*, 297−299.

(5) Lijinsky, W. *Mutat. Res.-Genetic Toxicol. Environ. Mutagen.* **1999**, *443*, 129−138.

(6) Spiegelhalder, B.; Preussmann, R. *Carcinogenesis* **1983**, *4*, 1147−1152.

(7) Mitch, W. A.; Sharp, J. O.; Trussell, R. R.; Valentine, R. L.; Alvarez-Cohen, L.; Sedlak, D. L. *Environ. Eng. Sci.* **2003**, *20*, 389−404.

(8) Challis, B. C.; Shuker, D. E. G.; Fine, D. H.; Goff, E. U.; Hoffman, G. A. *Iarc Publ.* **1982**, *41*, 11−20.

(9) Mirvish, S. S.; Sams, J. P.; Panigot, M.; Babcook, D. M. *Proc. Am. Assoc. Cancer Res.* **1985**, *26*, 114−114.

(10) Williams, D. L. H. *Nitrosation*; Cambridge University Press: New York, **1988**; p 214.

(11) Zolfigol, M. A.; Zebarjadian, M. H.; Chehardoli, G.; Keypour, H.; Salehzadeh, S.; Shamsipur, M. *J. Org. Chem.* **2001**, *66*, 3619−3620.

(12) Shapley, D. *Science* **1975**, *191*, 268−270.

(13) Herrmann, J.; Schuster, R. H. *Kautsch. Gummi Kunstst.* **1993**, *46*, 563−567.

(14) Schuster, R. H.; Wunsch, G.; Blume, A. *Kautsch. Gummi Kunstst.* **1994**, *47*, 651.

(15) Blume, A.; Wunsch, G.; Schuster, R. H. *Kautsch. Gummi Kunstst.* **1996**, *49*, 683−691.

(16) Diaf, A.; Beckman, E. J. *React. Polym.* **1995**, *25*, 89−96.

(17) Lui, H. L.; Conboy, J. J.; Hotchkiss, J. H. *J. Agric. Food Chem.* **1988**, *36*, 984−987.

(18) Tozawa, H.; Kawabata, T. *Bull. Jpn. Soc. Sci. Fish.* **1986**, *52*, 1969−1974.

(19) Tozawa, H.; Kawabata, T. *Nippon Suisan Gakkaishi* **1987**, *53*, 2209−2216.

(20) Tozawa, H.; Kawabata, T. *Nippon Suisan Gakkaishi* **1987**, *53*, 2259−2262.

(21) Tozawa, H.; Kawabata, T. *Nippon Suisan Gakkaishi* **1987**, *53*, 1449−1456.

(22) Mirvish, S. S.; Ramm, M. D.; Sams, J. P.; Babcook, D. M. *Cancer Res.* **1988**, *48*, 1095−1099.

(23) Skreiberg, O.; Kilpinen, P.; Glarborg, P. *Combust. Flame* **2004**, *136*, 501−518.

(24) Perry, R. A.; Siebers, D. L. *Nature* **1986**, *324*, 657−658.

(25) Mebel, A. M.; Diau, E. W. G.; Lin, M. C.; Morokuma, K. *J. Phys. Chem.* **1996**, *100*, 7517−7525.

(26) Mebel, A. M.; Lin, M. C. *Int. Rev. Phys. Chem.* **1997**, *16*, 249−266.

(27) Roose, T. R.; Hanson, R. K.; Kruger, C. H. *Proc. Int. Symp. Shock Tubes Waves* **1978**, *11*, 245.

(28) Zhao, Y. L.; Houk, K. N.; Olson, L. P. *J. Phys. Chem. A* **2004**, *108*, 5864−5871.

(29) Masuda, M.; Mower, H. F.; Pignatelli, B.; Celan, I.; Friesen, M. D.; Nishino, H.; Ohshima, H. *Chem. Res. Toxicol.* **2000**, *13*, 301−308.

(30) Becke, A. D. *J. Chem. Phys.* **1993**, *98*, 5648−5652.

(31) (a) Frisch, M. J.; Trucks, G. W.; Schlegel, H. B.; Scuseria, G. E.; Robb, M. A.; Cheeseman, J. R.; Montgomery, J. A., Jr.; Vreven, T.; Kudin, K. N.; Burant, J. C.; Millam, J. M.; Iyengar, S. S.; Tomasi, J.; Barone, V.; Mennucci, B.; Cossi, M.; Scalmani, G.; Rega, N.; Petersson, G. A.; Nakatsuji, H.; Hada, M.; Ehara, M.; Toyota, K.; Fukuda, R.; Hasegawa, J.; Ishida, M.; Nakajima, T.; Honda, Y.; Kitao, O.; Nakai, H.; Klene, M.; Li, X.; Knox, J. E.; Hratchian, H. P.; Cross, J. B.; Bakken, V.; Adamo, C.; Jaramillo, J.; Gomperts, R.; Stratmann, R. E.; Yazyev, O.; Austin, A. J.; Cammi, R.; Pomelli, C.; Ochterski, J. W.; Ayala, P. Y.; Morokuma, K.; Voth, G. A.; Salvador, P.; Dannenberg, J. J.; Zakrzewski, V. G.; Dapprich, S.; Daniels, A. D.; Strain, M. C.; Farkas, O.; Malick, D. K.; Rabuck, A. D.; Raghavachari, K.; Foresman, J. B.; Ortiz, J. V.; Cui, Q.; Baboul, A. G.; Clifford, S.; Cioslowski, J.; Stefanov, B. B.; Liu, G.; Liashenko, A.; Piskorz, P.; Komaromi, I.; Martin, R. L.; Fox, D. J.; Keith, T.; Al-Laham, M. A.; Peng, C. Y.; Nanayakkara, A.; Challacombe, M.; Gill, P. M. W.; Johnson, B.; Chen, W.; Wong, M. W.; Gonzalez, C.; Pople, J. A. *Gaussian 03*, revision C.02; Gaussian, Inc.: Wallingford, CT, 2004. (b) Certain commercial materials and equipment are identified in this paper in order to specify procedures completely. In no case does such identification imply recommendation or endorsement by the National Institute of Standards and Technology, nor does it imply that the material or equipment identified is necessarily the best available for the purpose.

(32) (a) Montgomery, J. A.; Frisch, M. J.; Ochterski, J. W.; Petersson, G. A. *J. Chem. Phys.* **1999**, *110*, 2822−2827. (b) See Gaussian thermochemistry white papers and technical notes, http://www. gaussian.com/g-whitepap/thermo.htm.

(33) Cossi, M.; Rega, N.; Scalmani, G.; Barone, V. *J. Comput. Chem.* **2003**, *24*, 669−681.